Electronic Supporting Information

Infiltrative coating of LiNi$_{0.5}$Co$_{0.2}$Mn$_{0.3}$O$_2$ microspheres with layer-structured LiTiO$_2$: Toward superior cycling performances for Li-ion batteries

Zongyi Wang, Sisi Huang, Baojun Chen, Hao Wu* and Yun Zhang*

College of Materials Science and Engineering, Sichuan University, Chengdu 610065, P. R. China

* Corresponding Author. E-mail: hao.wu@scu.edu.cn and y_zhang@scu.edu.cn

Part I: Experimental Section

Material Synthesis

Preparation of Ni$_{0.5}$Co$_{0.2}$Mn$_{0.3}$(OH)$_2$ Microspheres. Mesoporous Ni$_{0.5}$Co$_{0.2}$Mn$_{0.3}$(OH)$_2$ microspheres as precursors were first prepared by using a co-precipitation method. Typically, NiSO$_4$·6H$_2$O, MnSO$_4$·5H$_2$O, and CoSO$_4$·7H$_2$O were mixed with a molar ratio of Ni:Co:Mn=5:2:3 and with a concentration of 2.0 mol/L in distilledwater. The mixed solutionwas put into a CSTR (continuous stirred tank reactor) with a capacity of 2 L under N$_2$ atmosphere. Simultaneously, 2.0 mol/L solution of NaOH and 0.5 mol/L solution of NH$_4$OH as a chelating agent were separately fed into the continuous stirred tank reactor. The reaction was conducted at 50 ºC for 10 h, and the pH value in solution was kept at 11. Afterwards, the co-precipitated powders were filtered, washed and finally dried at 140 ºC for overnight to obtain the precursor Ni$_{0.5}$Co$_{0.2}$Mn$_{0.3}$(OH)$_2$ microspheres.

Pre-coating Procedure. A hydrolysis process of titanium salt was carried out to pre-coat $TiO_2 \cdot xH_2O$ on the $Ni_{0.5}Co_{0.2}Mn_{0.3}(OH)_2$ microspheres. In a typical preparation of 1 mol% coated sample (Ti:(Ni+Co+Mn) = 1:100 in molar ratio), 0.54 g $Ni_{0.5}Co_{0.2}Mn_{0.3}(OH)_2$ microspheres were firstly dispersed into 20 mL absolute ethanol, followed by addition of 0.020 g tetrabutyl titanate diluted in 0.4 mL absolute ethanol. The resulting suspension was kept stirring for 10 h to make sure the thorough mixing of microspheres with $Ti(OC_4H_9)_4$. Subsequently, a DI water-ethanol mixture (1:12 in volume) was added dropwise into the above suspension to trigger the hydrolysis reaction under vigorous stirring at ambient temperature. During the hydrolysis of $Ti(OC_4H_9)_4$, the precursor microspheres were gradually coated with the hydrolytic precipitate of hydrous titanium oxide. After stirring continuously for 24 h at the same temperature, the resulting products were washed with ethanol, and collected by centrifugation.

Synthesis of LiTiO_2-coated LiNi_{0.5}Co_{0.2}Mn_{0.3}O_2 Microspheres. After pre-coating treatment, the coated microspheres were dispersed in ethanol, and mixed with about 0.22 g Li_2CO_3. The amount of Li_2CO_3 is calculated by the following equation:

$$m_{Li2CO3} = 74g \cdot mol^{-1} \times [(n_{(Ni+Co+Mn)} + n_{Ti})/2]$$

The mixture was stirred under 80 ℃ until it was dry. Then, the blend was collected and sintered at 850 ℃ for 12 hours, with heat rate of 4 ℃·min⁻¹.

Synthesis of Pristine LiNi_{0.5}Co_{0.2}Mn_{0.3}O_2 Microspheres. For comparison, the uncoated pristine $LiNi_{0.5}Co_{0.2}Mn_{0.3}O_2$ microspheres were also prepared by using $Ni_{0.5}Co_{0.2}Mn_{0.3}(OH)_2$ and Li_2CO_3 as starting materials, and the sintering treatment was performed in the same procedure as described above.

Characterization

Crystal strucures of all samples were identified by powder X-ray diffraction measurement (XRD, D/Max-2000) using Cu Kα radiation in the 2θ range of 10 – 70° with a step of 0.02° and a scanning speed of 0.06° s⁻¹. Nitrogen sorption measurements were performed with Tristar 30 instrument (Micromeritics) to determine the specific surface area (SSA) and pore structure parameters of precursor $Ni_{0.5}Co_{0.2}Mn_{0.3}(OH)_2$ microspheres before and after $TiO_2 \cdot xH_2O$ pre-coating. X-ray photoelectron spectroscopy (XPS, AXIS Ultra DLD, Kratos)

was used to characterize valence state of surface elements and their content in samples. The morphologies of all samples were observed by scanning electron microscope (SEM, S-4800). Also, energy dispersive X-ray spectroscopy (EDS) was carried out as the attachment of SEM, with the acceleration voltage of 20 kV, in order to analyze the surface component of samples. Transmission electron microscope (TEM, JEM-100CX, JEOL, Japan) and high resolution TEM (HRTEM, JEM-2100F, JEOL, Japan) were employed to distinguish the coating layer and identify the interplanar spacing.

Electrochemical Measurements

The electrochemical properties of products were tested by CR2032 coin-type cell. The working electrodes were fabricated by dispersing 80 wt.% active materials, 15 wt.% black carbon (conductive materials), and 5 wt.% PVDF (binder) in N-methyl-2-pyrrolidone (NMP) solvent to form a homogeneous slurry. Afterwards, the slurry was coated on an Al foil current collector by an automatic coating machine (JFA-Ⅱ, Tianjin Yonglida laboratory equipment Co., LTD.), and then dried at 120 ℃ for 10 h in a vacuum oven. All electrodes were cut into disks with a diameter of 14 mm, the average mass loading of which was about 5.0 mg·cm^{-2}. Subsequently, CR-2032 coin-type cells were assembled in an argon-filled glove box by utilizing the above prepared disks as cathode, metal lithium foils as anode, polypropylene micro-porous films (Celgard 2400) as separator, and 1M LiPF$_6$ dissolved in a mixture of ethylene carbonate (EC) and dimethyl carbonate (DMC) and diethyl carbonate (DEC) (1:1:1 in volume) as electrolyte. Galvanostatic charge and discharge tests were conducted in a potential range of 3.0–4.4 V (*vs.* Li/Li$^+$) at 25 and 55 °C using a battery system (Neware CT-3008W battery tester, China). The Electrochemical impedance spectroscopy (EIS) tests were performed by the CHI600D electrochemical workstation in the frequency range of 100 kHz to 10 mHz with the scanning rate of 0.1 mV/s.
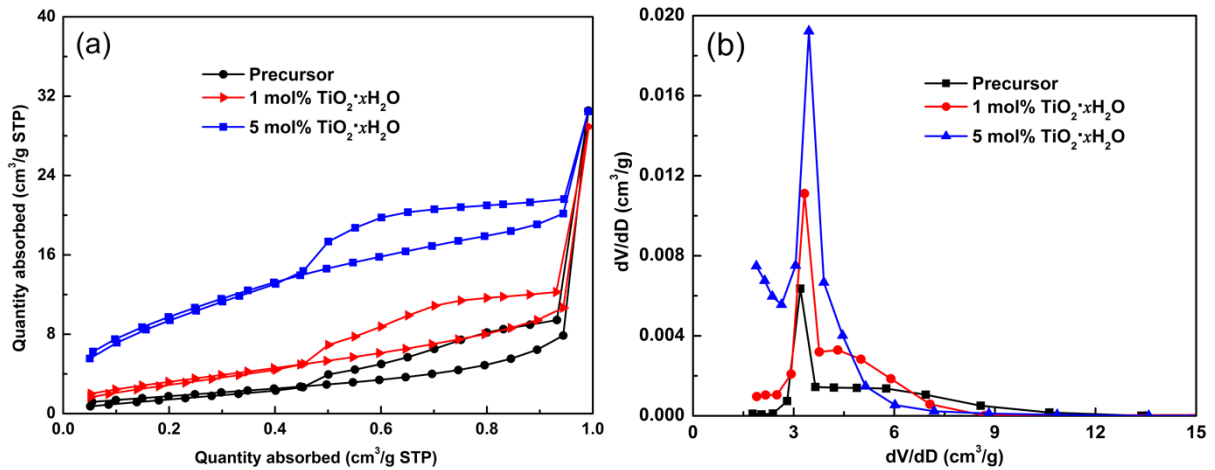
Part II: Supporting Figures and Tables

Fig. S1 (a) N_2 adsorption/desorption isotherms and (b) pore size distribution curves of precursor $Ni_{0.5}Co_{0.2}Mn_{0.3}(OH)_2$ microspheres before and after 1 and 5 mol% $TiO_2 \cdot xH_2O$ pre-coating

As shown in Fig. S1a, the precursor $Ni_{0.5}Co_{0.2}Mn_{0.3}(OH)_2$ microsphere displays the type IV isotherm with a clear hysteresis loops, indicating the presence of mesoporous structure. The Brunauer-Emmett-Teller (BET) surface area of the precursor was calculated to be 6.9 m^2/g, while its Barrett-Joyner-Halenda (BJH) pore size distribution derived from the desorption isotherm centered at around 14.1 nm, attributing to the interstitial spacings between the stacked flake-like primary particles. After pre-coating with 1 and 5 mol% $TiO_2 \cdot xH_2O$, the pore size of the precursor decreased to be 9.2 and 4.8 nm, respectively, accompanied by increased BET surface are of 12.7 and 37.9 m^2/g, respectively, mainly due to the uniform and complete deposition of $TiO_2 \cdot xH_2O$ into the pores throughout the entire microspheres.

Table S1. Summary of BET specific surface area and BJH pore structure parameters

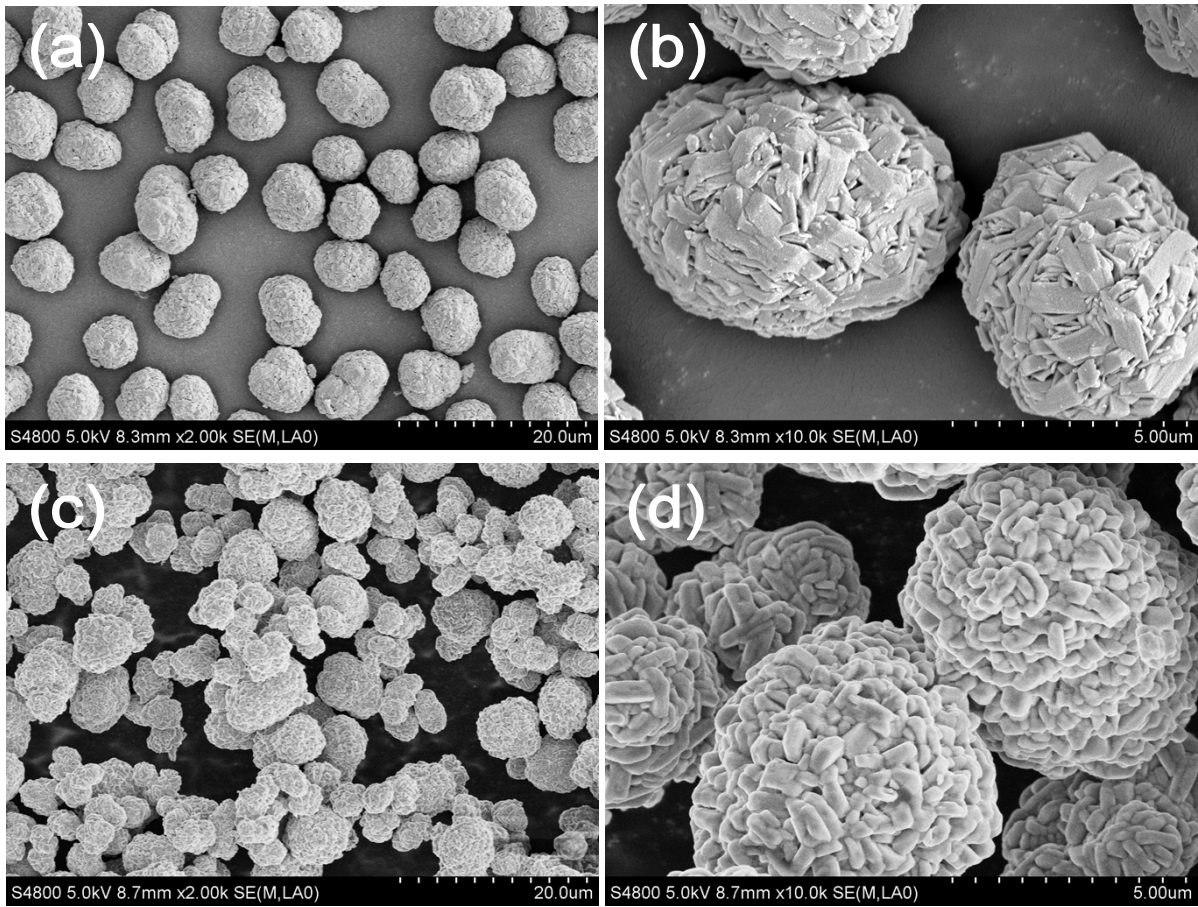| Sample	BET SSA (m^2/g)	Average pore size (nm)	Pore volume (cm^3/g)
Precursor	6.9	14.1	0.047
1 mol% $TiO_2 \cdot xH_2O$ coating	12.7	9.2	0.044
5 mol% $TiO_2 \cdot xH_2O$ coating	37.9	4.8	0.042

Fig. S2 SEM images of (a and b) $Ni_{0.5}Co_{0.2}Mn_{0.3}(OH)_2$ microspheres and (c and d) corresponding pristine LNCM product at low and high magnification
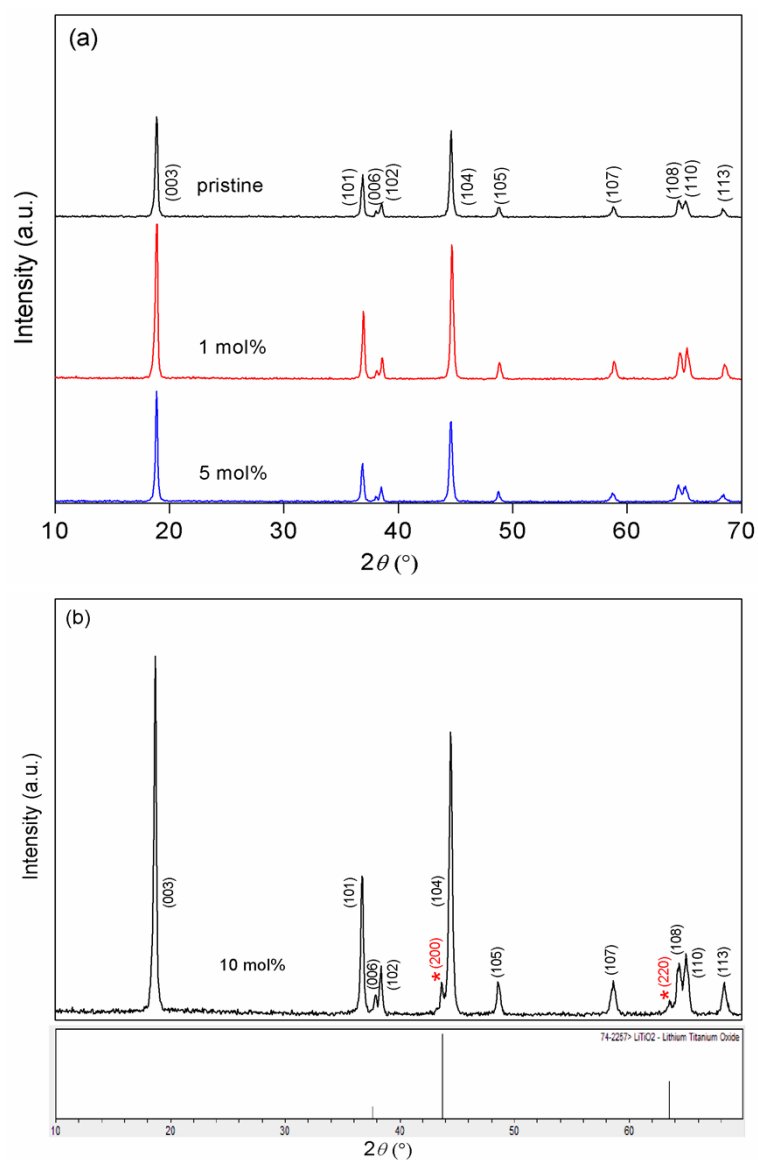
Fig. S3 XRD patterns of (a) pristine and LiTiO$_2$-coated LNCM product (1 and 5 mol% coating content) and (b) 10 mol% LiTiO$_2$-coated LNCM product

Table S2. Riveted cell refinement results of the pristine and LiTiO$_2$-coated LNCM products

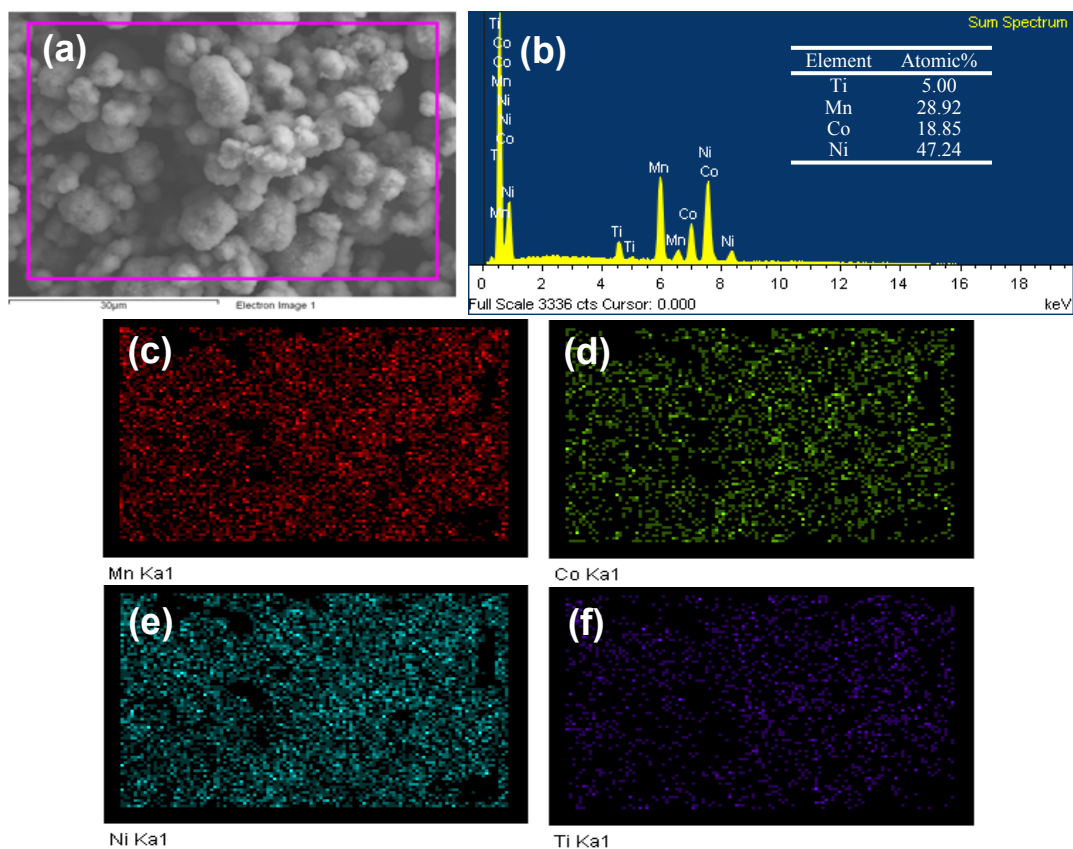| Sample	Space group	a (Å)	Vol. (Å^3)
Pristine	*R-3m*	2.86118	100.66
1 mol% coated LNCM	*R-3m*	2.86203	100.89
5 mol% coated LNCM	*R-3m*	2.86316	101.24

Fig. S4 (a) SEM image and (b) EDS spectrum of 5 mol% LiTiO$_2$-coated LNCM. (c–f) EDS dot-mapping results of Mn (c), Co (d), Ni (e), and Ti (f)
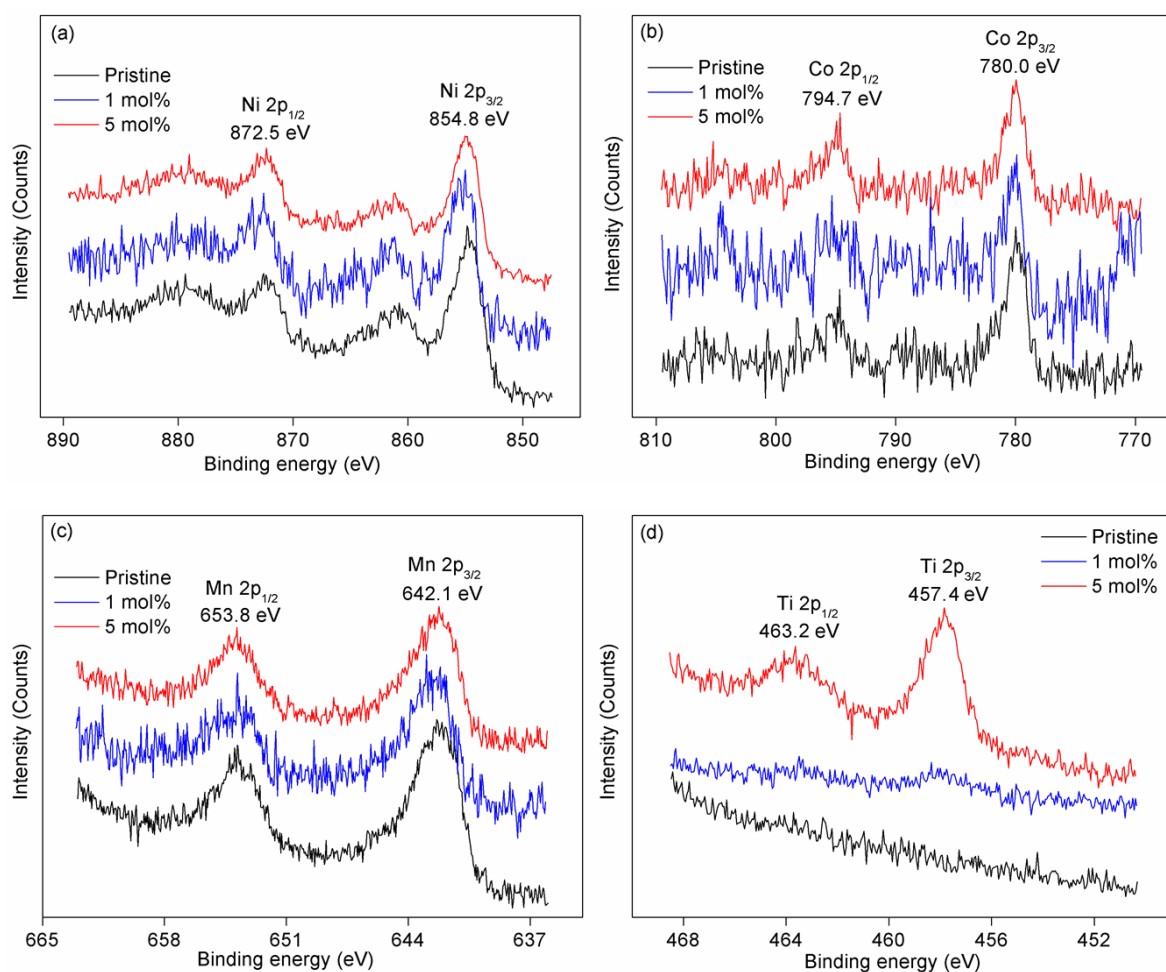
Fig. S5 XPS spectra for (a) Ni, (b) Co, (c) Mn, and (d) Ti elements of pristine, 1, and 5 mol%

LiTiO$_2$-coated LNCM products

Table S3. Summary of atomic ratio of Ti to (Ni+Co+Mn) of products determined from XPS
and from precursor applied in the synthetic process.[a]

Samples	Ti:(Ni+Co+Mn)	
	XPS results	Starting ratio
Pristine	0:(49+19+32)	0:(50+20+30)
1 mol%	3:(51+15+34)	1:(50+20+30)
5 mol%	14:(53+12+36)	5:(50+20+30)

[a] The results of XPS element qualification was calculated and analyzed according to the method described
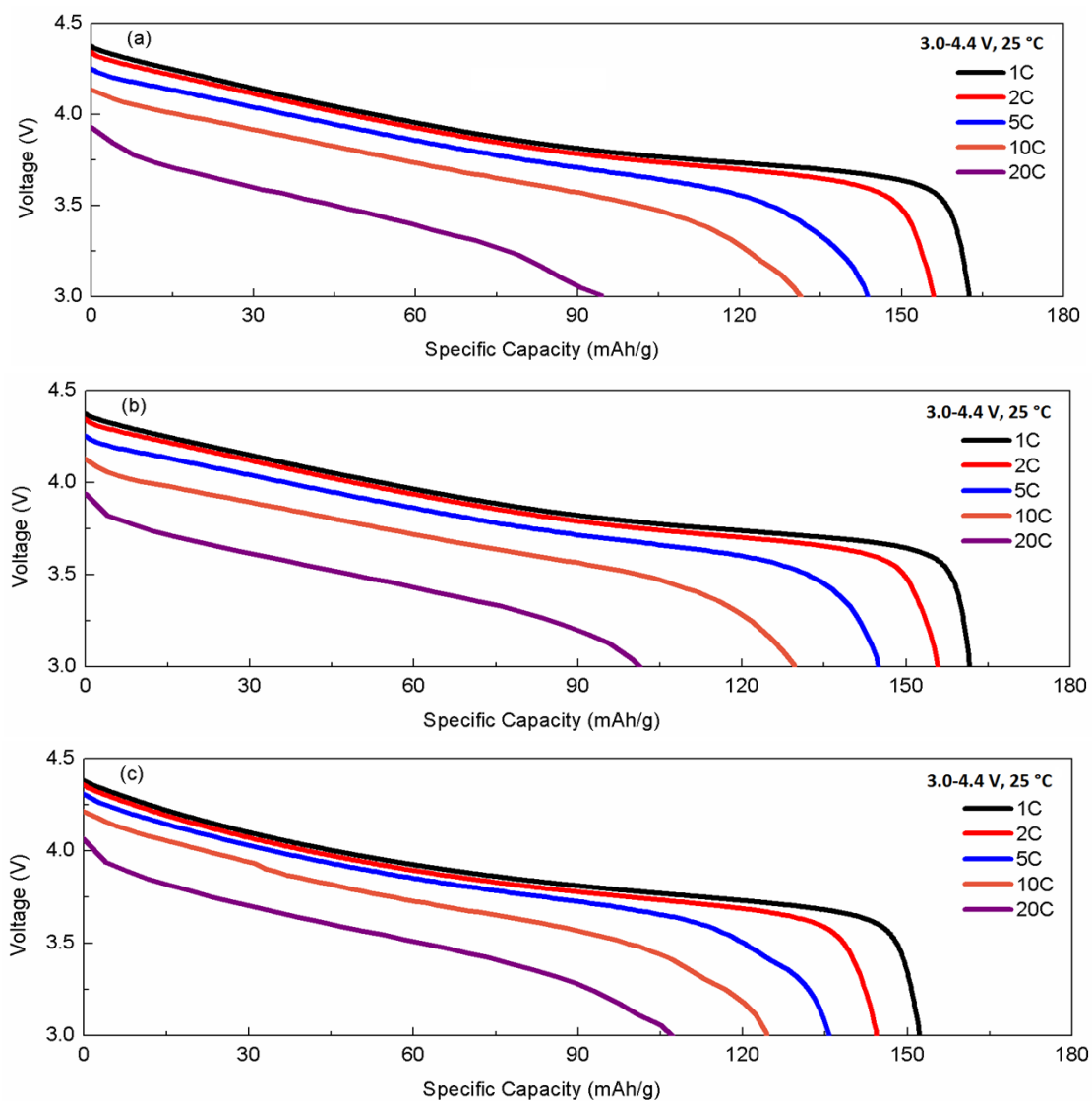in the literature.[S1,2]

Fig. S6 Typical discharge voltage-capacity profiles of (a) pristine, (b) 1, and (c) 5 mol%

LiTiO$_2$-coated LNCM products at variable current rate of 1, 2, 5, 10, and 20 C

Table S43. Discharge capacity of the products at varibale current rate

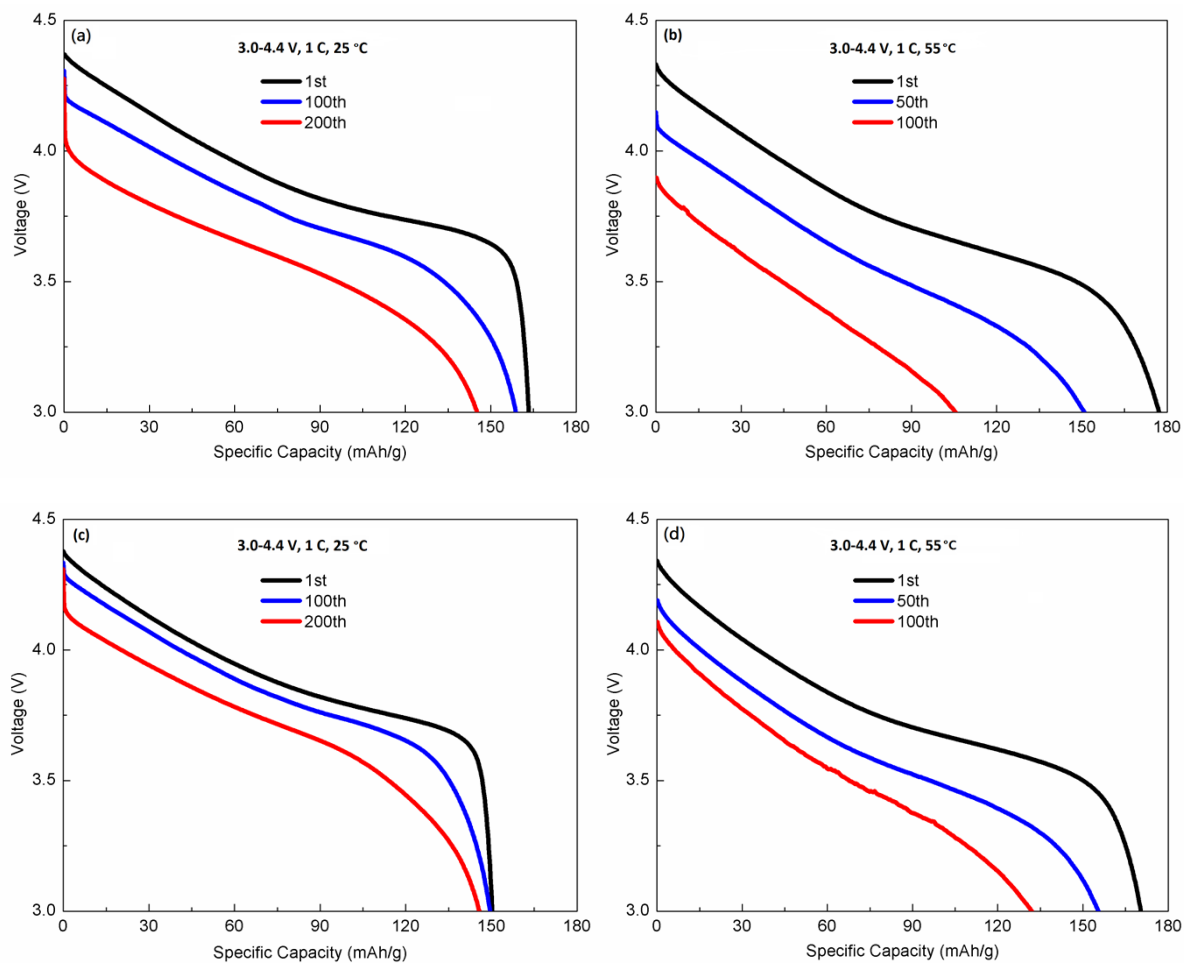| Samples	Discharge capacity (mA h/g)					
	1 C	2 C	5 C	10 C	20 C	Back to 1 C
Pristine	163.8	155.8	144.9	131.4	94.4	163.3
1 mol%	162.4	155.9	143.7	129.6	101.3	161.7
5 mol%	151.3	144.4	135.8	124.9	107.2	150.5

Fig. S7 Typical discharge voltage-capacity profiles of (a and b) 1 and (c and d) 5 mol%

LiTiO$_2$-coated LNCM at the different cycle numbers under 25 (a and c) and 55 ℃ (b and d)

Table S54. Capacity retention of the products after cycling at 1 C under 25 and 55 ℃

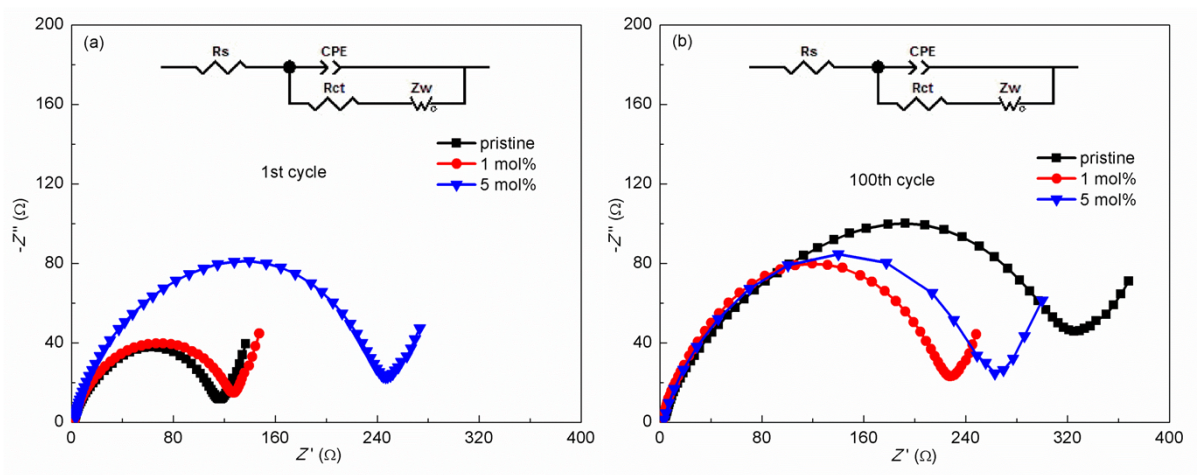| Samples	25 ℃			55 ℃		
	Pristine	1 mol%	5 mol%	Pristine	1 mol%	5 mol%
Initial capacity (mA h/g)	167.4	163.3	150.1	181.1	177.1	170.7
The 100th capacity (mA h/g)	142.5	158.7	149.5	51.2	106.5	131.5
The 200th capacity (mA h/g)		145.4	145.9			
Final capacity retention (%)	85.1	89.1	97.2	28.3	60.1	77.0

Fig. S8 Nyquist plots of the pristine and LiTiO$_2$-coated LNCM electrodes at a charge state of 4.4 V in the (a) 1st and (b) 100th cycle at 1 C under 25 °C; Insets in (a) and (b) show the equivalent circuit used to fit the measured impedance spectra

Table S65. The values of R_s and R_{ct} for pristine and LiTiO$_2$-coated LNCM products in the 1st and 100th cycle at 1 C under 25 °C

Samples	1st cycle		100th cycle	
	R_s (Ω)	R_{ct} (Ω)	R_s (Ω)	R_{ct} (Ω)
Pristine	1.94	109.3	2.64	340.5
1 mol%	1.83	109.4	1.86	211.6
5 mol%	2.16	218.4	2.52	223.8

As described in Table S65, the R_s values representing the solution resistance, for all electrodes have no distinct changes during cycling process, which can be ascribed to the slow decomposition of electrolyte solution with cycles.[S3] Contrarily, all the three electrodes demonstrated increasing R_{ct} values, which refers to charge transfer resistance,[S3] upon continuous cycling. This phenomenon can be associated to the fact that the thicker solid electrolyte interphase (SEI) film on the electrode surface increased the electrochemical kinetics obstacles. It can be seen that the increase of R_{ct} values between the pristine and coated

electrodes became different as the cycle reached to the 100th. The ever-growing interface reaction between the electrolyte and electrode can be significantly responsible for the increase of R_{ct} values. Specifically, the R_{ct} value of the pristine LNCM electrode increased from 109.3Ω at the 1st cycle to 340.5 Ω at the 100th cycle, whereas the R_{ct} values of the 1 and 5 mol% LiTiO$_2$-coated electrodes only increased from 109.4 and 218.4 Ω at the 1st cycle to 211.6 and 223.8 Ω at the 100th cycle, respectively. Clearly, the LiTiO$_2$-coated electrodes showed much smaller resistance increase than that of the pristine one. This fact suggests that LiTiO$_2$ acts as a role of a protective layer to restrain the oxidation of electrolyte and structural destruction of electrode material at high cut-off voltage so as to avoid the over-rapid thickening of electronically insulating SEI film,[S4] and decrease the rate of impedance increase during long-term cycling.
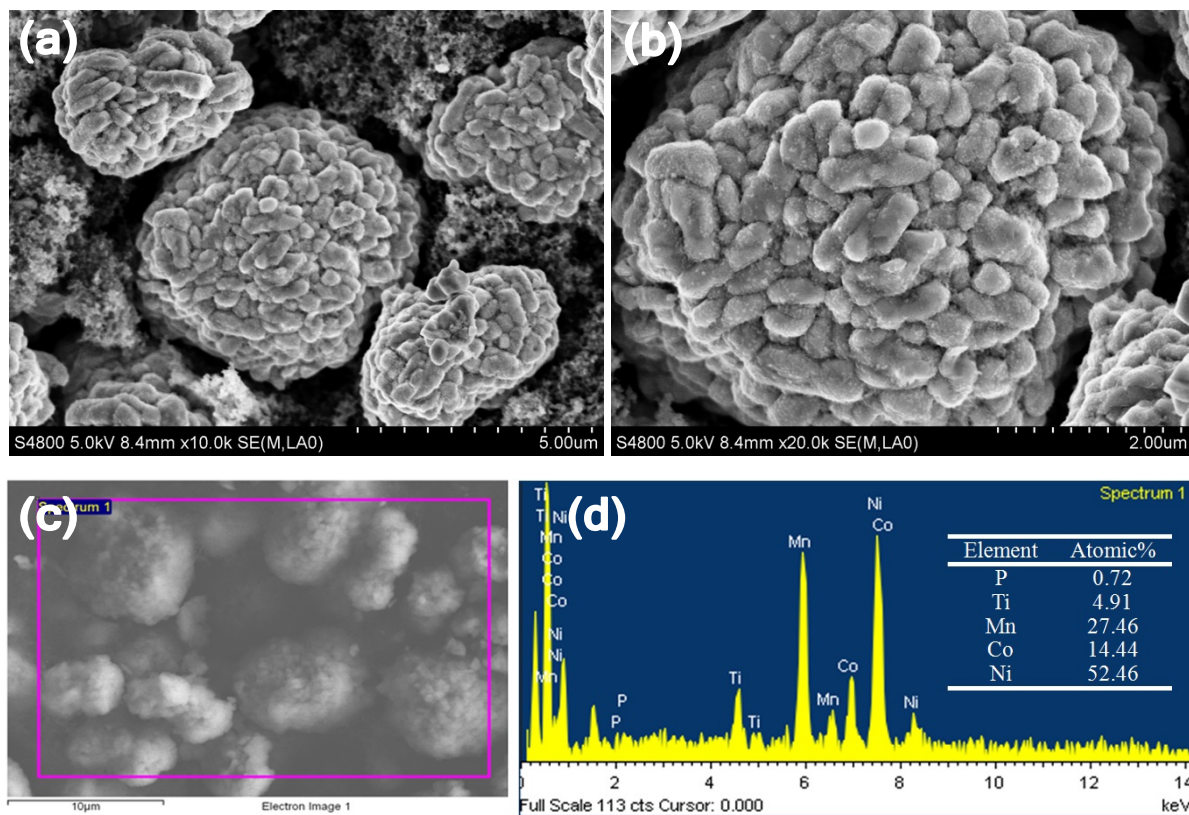
Element	Atomic%
P	0.72
Ti	4.91
Mn	27.46
Co	14.44
Ni	52.46

Fig. S9 SEM images (a and b) and EDS spectrum (c and d) of the 5 mol% LiTiO$_2$-coated LNCM electrode after 100 cycles at 1 C under 25 ºC

Reference

[S1]. B. Philippe, R. Dedryvere, J. Allouche, F. Lindgren, M. Gorgoi, H. Rensmo, D. Gonbeau and K. Edstrom, *Chem. Mater.*, 2012, **24**, 1107.

[S2]. J. Lu, Q. Peng, W. Y. Wang, C. Y. Nan, L. H. Li and Y. D. Li, *J. Am. Chem. Soc.*, 2013, **135**, 1649.

[S3]. J. M. Zheng, X. B. Wu and Y. Yang, *Electrochim. Acta*, 2011, **56**, 3071.

[S4]. S. K. Martha, J. Nanda, G. M. Veith and N. J. Dudney, *J. Power Sources*, 2012, **216**, 179.